PHYSICAL REVIEW D **74,** 115012 (2006)

Classical trajectories and quantum supersymmetry

Piotr Korcyl

M. Smoluchowski Institute of Physics, Jagellonian University Reymonta 4, 30-059 Kraków, Poland

(Received 11 October 2006; published 18 December 2006)

We analyze a supersymmetric system with four flat directions. We observe several interesting properties, such as the coexistence of the discrete and continuous spectrum in the same range of energies. We also solve numerically the classical counterpart of this system. A similar analysis is then done for an alike, but nonsupersymmetric, system. The comparison of these classical and quantum results may serve as a suggestion about classical manifestations of supersymmetry.

DOI: 10.1103/PhysRevD.74.115012 PACS numbers: 12.60.Jv

I. INTRODUCTION

Great interest has been recently put on the supersymmetric Yang-Mills quantum mechanics (SYMQM), which results from a dimensional reduction of the supersymmetric Yang-Mills field theories to a single point in space. The use of simple numerical methods gives a good understanding of the $N = 2$, $D = 2$, and $D = 4$ models [1–3]. The ultimate goal of such an analysis is the $D = 10$, SU($N \to \infty$) model, which is conjectured to be in relation with the M-theory [4].

The system addressed here was used by de Wit, Lüscher, and Nicolai in [5,6] as a simplified model of the supermembrane Hamiltonian in an extensive discussion on stability of supermembranes, structures present in the M-theory. It is one of the simplest supersymmetric models with flat directions. It thus contains several interesting properties of SYMQM, such as the coincidence of the discrete and continuous spectrum. The aim of this paper is to analyze in detail this system with the method proposed by Wosiek [1] and to compare it with an analogous, but nonsupersymmetric, model. The latter was also already described in the literature on both, classical and quantum [7,8], levels. It has an interesting feature, all its eigenstates are localized, even though the potential is zero on an unbounded set.

The paper is composed as follows. We start by introducing the quantum systems: the nonsupersymmetric one and the supersymmetric one, and we continue by presenting their classical counterparts. The comparison in the quantum regime is based on the analysis of numerical spectra, therefore we proceed by describing the method used for calculating spectra, and then give a detailed study of all symmetries present in these systems in order to fully understand the degeneracies which may appear. Consequently, we discuss the results of this comparison. Finally, we turn to the classical regime and analyze the classical bosonic and supersymmetric trajectories. Comparing them enables us to rediscover the differences between quantum systems on the classical level.

II. DESCRIPTION OF THE SYSTEM

In this chapter we introduce the Hamiltonians of the considered models; first the quantum, then the classical one. In the following, the nonsupersymmetric system will be called bosonic, because it contains only bosonic degrees of freedom.

A. Quantum systems

The quantum bosonic Hamiltonian has the form

$$\hat{H}_{\text{bosonic}} = \hat{p}_x^2 + \hat{p}_y^2 + \hat{x}^2\hat{y}^2. \tag{1}$$

The potential x^2y^2 has four flat directions. Usually, we expect that systems with potentials equal to zero on an unbounded set, have continuous spectrum. Nevertheless, in our case, the spectrum turns out to be exclusively discrete due to the quantum fluctuations in the transverse directions. Let us consider a particle moving in one of the valleys, say $x > 0$. The transverse potential is the potential of a harmonic oscillator with an equilibrium position at $y = 0$ and frequency proportional to the distance from the center $\omega \sim |x|$. The zero-mode energy of such fluctuations increases linearly with $|x|$, when the particle is moving deep into the valley. Therefore, the particle is exposed to an effective potential barrier, which prevents it from escaping. We will now recall [8] the solution of the stationary Schrödinger equation in the Born-Oppenheimer approximation in order to explicitly show the above. The energy of a quantum harmonic oscillator of frequency $|x|$ is equal to

$$E_x = |x|(n_y + \tfrac{1}{2}).$$

The wave function can be written as a product of two functions,

$$\Psi(x, y) = \alpha(x)\beta_{x,n_y}(y),$$

where $\alpha(x)$ accounts for the onward motion, and $\beta_{x,n_y}(y)$ describes the transverse harmonic fluctuations,

$$\left(-\frac{\partial^2}{\partial y^2}+x^2y^2\right)\beta_{x,n_y}(y)=2|x|\left(n_y+\frac{1}{2}\right)\beta_{x,n_y}(y).$$

Thus, $\beta_{x,n_y}(y)$ is a well-known eigenfunction of quantum harmonic oscillator,

$$\beta_{x,n_y}(y)=(\sqrt{\pi}2^{n_y}n_y!)^{-1/2}H_{n_y}(\sqrt{2|x|}y)e^{-y^2|x|}.$$

$\alpha(x)$ satisfies a stationary Schrödinger equation:

$$\left(-\frac{\partial^2}{\partial x^2}+2|x|\left(n_y+\frac{1}{2}\right)\right)\alpha(x)=E_{n_x,n_y}\alpha(x).$$

We now proceed independently for $x>0$ and $x<0$. Let us introduce a new variable z:

$$z=\left(n_y+\frac{1}{2}\right)^{1/3}\left(x-\frac{E}{2n_y+1}\right).$$

The equation for $\alpha(x)$ can be now rewritten in this variable as

$$\ddot{\alpha}(z)-2z\alpha(z)=0.$$

This is the Airy equation. Its solutions are even and odd Airy's functions. In order to obtain a full solution we have to match together solutions from $x>0$ and $x<0$ valleys. This gives us the condition of energy quantization, which turns out to be the equation for the zeros of Airy's function

$$Ai\left(\frac{-E}{(2n_y+1)^{2/3}}\right)=0.$$

This condition has a straightforward interpretation. The spectrum is discrete, because the Airy's functions are analytic and therefore have countable many zeros on the real axis. The few first approximate eigenenergies are shown in Table II, together with some exact ones. The compatibility is within 7%. The assumption, that the particle moves only in one of the valleys, breaks the space symmetries of the system, so the approximated energies will not have degeneracies.

The quantum supersymmetric Hamiltonian has the form

$$\hat{H}_{\text{susy}}=\hat{p}_x^2+\hat{p}_y^2+\hat{x}^2\hat{y}^2+(\hat{x}+i\hat{y})f^\dagger+(\hat{x}-i\hat{y})f, \quad (2)$$

where $f^\dagger$ and f are the fermionic creation and annihilation operators, respectively. The operator $f^\dagger f$ does not commute with the Hamiltonian (2), so the fermionic occupation number is not a good quantum number and cannot be used to label the eigenstates. This generates nonvanishing, nondiagonal matrix elements in the fermionic occupation number representation.

There exists one supersymmetry generator,

$$\hat{Q}=\hat{Q}^\dagger=\frac{1}{\sqrt{2}}((\hat{p}_x+i\hat{p}_y)f+(\hat{p}_x-i\hat{p}_y)f^\dagger+\hat{x}\,\hat{y}[f^\dagger,f]), \quad (3)$$

such that

$$\hat{H}=\{\hat{Q}^\dagger,\hat{Q}\},$$

and

$$[\hat{H},\hat{Q}]=0.$$

Although the supersymmetry concerns particles—bosons and fermions—it is sometimes useful to think about the fermionic degree of freedom as an equivalent spin projection on the OZ axis. In this language the Hamiltonian and the supersymmetry generator take the form

$$\hat{H}_{\text{susy}}=\hat{p}_x^2+\hat{p}_y^2+\hat{x}^2\hat{y}^2+\sigma_x\hat{x}-\sigma_y\hat{y},$$

$$\hat{Q}=\hat{Q}^\dagger=\frac{1}{\sqrt{2}}(\hat{p}_x\sigma_x+\hat{p}_y\sigma_y+\hat{x}\,\hat{y}\,\sigma_z).$$

The analytic analysis of the system (2) is difficult because of the mentioned nondiagonal matrix elements in the fermionic occupation number representation. We can nevertheless extract some useful information by analyzing a simpler and more regular model. It will enable us to demonstrate the effect of coexistence of the discrete and continuous spectrum in the same range of energies. Let us consider the Hamiltonian

$$\hat{H}_{\text{model}}=\hat{p}_x^2+\hat{p}_y^2+\hat{x}^2\hat{y}^2+\hat{x}[f^\dagger,f]. \quad (4)$$

We will use now, as in the purely bosonic case, the Born-Oppenheimer approximation. It has to be noted that, although the model Hamiltonian (4) does not have the space symmetries present in the original system (2), it does not spoil its usefulness, because the approximation breaks these symmetries anyway. Let us consider the motion in one of the valleys, say $x>0$. The transverse potential is a potential of a quantum supersymmetric harmonic oscillator of frequency $\omega\sim|x|$. The Hamiltonian of such an oscillator is [9]

$$\hat{H}_{\text{susy oscillator}}=\frac{1}{2}\hat{p}_y^2+\frac{1}{2}|x|^2\hat{y}^2+\frac{|x|}{2}[f^\dagger,f].$$

Its energies depend on one quantum number n and are equal

$$E_n=|x|n.$$

Similarly to the bosonic case, we write the wave function as a product of two functions:

$$\Psi(x,y)=\alpha(x)\beta_{x,n}(y),$$

where $\alpha(x)$ accounts for the onward motion and $\beta_{x,n}(y)$ fulfills the equation

$$\left(-\frac{\partial^2}{\partial y^2}+x^2y^2-|x|[f,f^\dagger]\right)\beta_{x,n}(y)=2n|x|\beta_{x,n}(y).$$

This gives us the equation on $\alpha(x)$:

$$\left(-\frac{\partial^2}{\partial x^2}+2n|x|\right)\alpha_n(x)=E\alpha_n(x). \tag{5}$$

From the form of (5) we can conclude that the spectrum has two coexisting parts: a continuous part for $n=0$ and a discrete one for $n\geq 1$. The zero energy of the zero modes enables the particle to penetrate the valley to any depth. The same effect is present in the original system (2), so it seems that (4) is a good candidate to model this feature.

A detailed study of spectra of both bosonic and supersymmetric quantum models is described later on.

B. Classical systems

The classical bosonic Hamiltonian has the form

$$H_{\text{boz}}=p_x^2+p_y^2+x^2y^2. \tag{6}$$

We easily find the equations of motion

$$\begin{aligned}\dot{x}&=2p_x, & \dot{y}&=2p_y,\\ \dot{p}_x&=-2xy^2, & \dot{p}_y&=-2yx^2.\end{aligned} \tag{7}$$

These equations imply that particles which move exactly along the coordinate axes have a constant momentum component along these axes. This, of course, corresponds to a free motion in these directions. We will show later that any other trajectory is bounded in the sense that it always returns to the center of the potential. This property of the x^2y^2 potential can be easily investigated using the so-called hyperbolic billiard. The authors of the article [10] have considered a classical, free, spinless particle moving as a free particle in a bounded set,

$$D=\{(x,y)|x\geq 0\wedge y\geq 0\wedge y\leq 1/x\},$$

which is an idealized version of the potential in (6). They showed that such a particle cannot escape through the valleys, it always turns back. They also proved that it is possible to systematically find all closed orbits. Every orbit can be unambiguously labeled by a set of symbols which correspond to reflection from particular walls of the potential. Such a list of all orbits is particularly useful in the semiclassical calculations by Feynman integrals.

The classical equations of motion of the supersymmetric system can be obtained from the quantum Hamiltonian (2) using the Ehrenfest's equation for mean values:

$$\begin{aligned}&\dot{x}=2p_x, \quad \dot{y}=2p_y, \quad \dot{p}_x=-2xy^2-2S_x,\\ &\dot{p}_y=-2yx^2+2S_y, \quad \dot{S}_x=-2yS_z,\\ &\dot{S}_y=-2xS_z, \quad \dot{S}_z=2xS_y+2yS_x.\end{aligned} \tag{8}$$

Equations (8) can also be derived in a different way. As was shown in the paper by Berezin [11], for the description of classical dynamics of a nonrelativistic particle with spin $\frac{1}{2}$ one needs an enriched phase space. This description uses three, anticommuting, dynamical variables ξ_k which belong to a Grassmann algebra G_3 with three generators:

$$\xi_k\xi_l+\xi_l\xi_k=0, \qquad k,l=1,2,3.$$

In particular, $\xi_k^2=0$. We can use relations between quantum spin projection operators with their classical counterparts expressed in terms of ξ. We thus obtain a classical form of the supersymmetric Hamiltonian:

$$H_{\text{susy}}=p_x^2+p_y^2+x^2y^2-i(x\epsilon_{xlm}-y\epsilon_{ylm})\xi_l\xi_m.$$

The time dependence of the dynamical variables can be derived from the Hamilton equations: $\frac{dq}{dt}=\frac{\partial H}{\partial p}$, $\frac{dp}{dt}=-\frac{\partial H}{\partial q}$, $\frac{d\xi_i}{dt}=iH\frac{\overleftarrow{\partial}}{\partial\xi_i}$, where $q=x,y$ and $p=p_x,p_y$. The appearance of the imaginary i in the classical equations is inherently related to the nature of the Grassmann variables.

$$\begin{aligned}&\dot{x}=2p_x, \quad \dot{y}=2p_y, \quad \dot{p}_x=-2xy^2+i\epsilon_{xlm}\xi_l\xi_m,\\ &\dot{p}_y=-2yx^2-i\epsilon_{ylm}\xi_l\xi_m, \quad \dot{\xi}_1=-2y\xi_3,\\ &\dot{\xi}_2=-2x\xi_3, \quad \dot{\xi}_3=2x\xi_2+2y\xi_1.\end{aligned} \tag{9}$$

It is useful to replace the Grassmann variables ξ_k in these equations by the spin projections S_k, which are the physical observables:

$$S_k=-\frac{i}{2}\epsilon_{klm}\xi_l\xi_m, \qquad \dot{S}_k=-\frac{i}{2}\epsilon_{klm}(\dot{\xi}_l\xi_m+\xi_l\dot{\xi}_m).$$

We get rid of the time derivatives $\dot{\xi}_k$ using the equations of motion (9). The equations for S_k close and we get the already obtained set of Eqs. (8). In this language, the Hamiltonian takes the form

$$H_{\text{susy}}=p_x^2+p_y^2+x^2y^2+2xS_x-2yS_y. \tag{10}$$

Furthermore, Eq. (10) can be rewritten in a form where the spin precession is evident. To this end we define a vector field, which is space dependent:

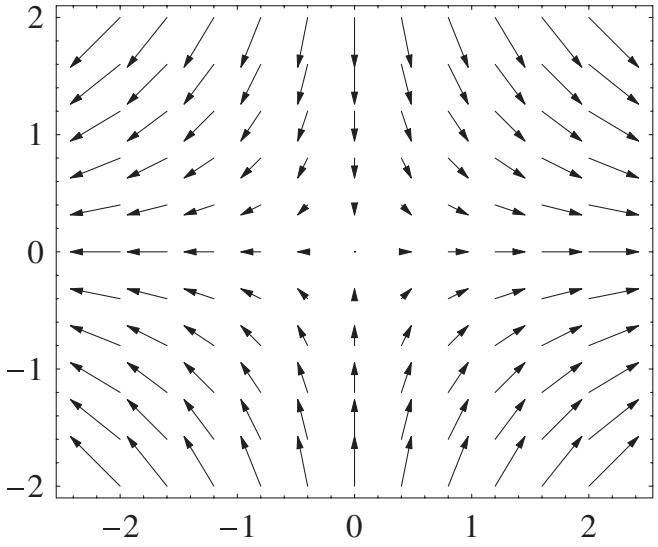

FIG. 1. Vector field $\vec{V}$ about which the spin rotates.

$$\vec{V} = (V_x, V_y, V_z) = (2x, -2y, 0).$$

Then

$$H_{\text{susy}} = p_x^2 + p_y^2 + x^2y^2 + \vec{S} \cdot \vec{V},$$

which manifestly shows the precession effect. It is noteworthy that such a field is tangent to the contour line of the potential x^2y^2, see Fig. 1.

III. QUANTUM MECHANICS ON PC

A numerical analysis of quantum systems can be easily carried out in an eigenbasis of occupation number operators, a so-called Fock basis [1]. The occupation number operator can be written as $a^\dagger a$, where $a^\dagger$ and a are standard bosonic creation and annihilation operators, respectively. They fulfill well-known commutation relations:

$$[a_p, a_q] = [a_p^\dagger, a_q^\dagger] = 0, \qquad [a_p, a_q^\dagger] = \delta_{pq}. \tag{11}$$

p and q in (11) are indices which label the bosonic degrees of freedom. Particularly, the nonsupersymmetric system (1) has two bosonic degrees of freedom, labeled x and y. Thus, a basis state is described by two integers

$$|m, n\rangle = \frac{1}{\sqrt{n!m!}}(a_x^\dagger)^m(a_y^\dagger)^n|0\rangle, \qquad m, n \geq 0. \tag{12}$$

Of course, in a numerical analysis it is impossible to use an infinite basis, so a cutoff, N_{cut}, is needed, which limits the number of basis states. There are many ways to introduce such a cutoff. One of them, called a square cutoff, is to limit independently the maximal number of occupation for each of two degrees of freedom by $\sqrt{N_{\text{cut}}}$.

The momentum and position operators can be expressed by creation and annihilation operators in the following way:

$$\begin{aligned} x &= \frac{1}{\sqrt{2}}(a_x + a_x^\dagger), \qquad p_x = \frac{1}{i\sqrt{2}}(a_x - a_x^\dagger), \\ y &= \frac{1}{\sqrt{2}}(a_y + a_y^\dagger), \qquad p_y = \frac{1}{i\sqrt{2}}(a_y - a_y^\dagger). \end{aligned} \tag{13}$$

The action of the Hamiltonian, which is an operator function of (13), is straightforward in the Fock basis. We can easily calculate its matrix elements. The eigenenergies of a quantum system belong to a set of eigenvalues of the Hamiltonian matrix, and the eigenstates are the eigenvectors of this matrix.

In the supersymmetric case we must introduce fermionic creation and annihilation operators, f and $f^\dagger$, which fulfill the anticommutation relations:

$$\{f_p, f_q\} = \{f_p^\dagger, f_q^\dagger\} = 0, \qquad \{f_p, f_q^\dagger\} = \delta_{pq}, \tag{14}$$

where p and q are indices which describe the fermionic degrees of freedom. In general, in order to ensure the relations (14), one uses a construction by Jordan and Wigner [12]. In a case of only one fermionic degree of freedom it is not necessary. The fermionic occupation number operator $f^\dagger f$, with two eigenvalues 0 i 1, permit to label the basis states by a third quantum number:

$$\begin{aligned} |m, n, k\rangle &= \frac{1}{\sqrt{n!m!}}(a_x^\dagger)^m(a_y^\dagger)^n(f^\dagger)^k|0\rangle, \\ m, n \geq 0, &\qquad k = 0, 1. \end{aligned} \tag{15}$$

The above method allows also to verify the reliability of numerical results. The rate of convergence of eigenenergies with an increasing N_{cut} is a simple criterion. For example, we can assume that the convergence is reached when a relative change of the energy between consecutive N_{cut} is less than 1% of its absolute value. For the bosonic ground state this happens for $N_{\text{cut}} > 100$. The excited states have a worse convergence so all the following results were obtained for $N_{\text{cut}} = 400$. The dependence of the energy of the bosonic ground state on the cutoff is shown in Fig. 2 with a solid line. This dependence provides us also with an additional information on the character of the quantum state. Particularly, as it will be described later, it enables one to decide whether the state belongs to the discrete spectrum or to the continuous one.

Another criterion of reliability is supplied by the spatial probability distributions. One can assume that the convergence is reached when for consecutive cutoffs, N_{cut} and N'_{cut}, the probability $P(x)$ of finding the particle at the point x fulfills the inequality,

$$\max_{x \in I} \frac{|P_{N_{\text{cut}}}(x) - P_{N'_{\text{cut}}}(x)|}{P_{N_{\text{cut}}}(x)} < \epsilon,$$

where I is an interval on which the distributions are calculated. Figure 3 shows a cross section along the OX axis of such distribution for the bosonic ground state for different

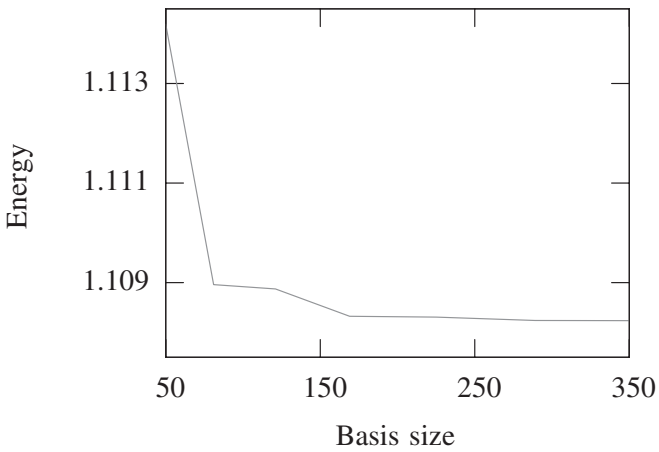

FIG. 2. The dependence of the ground state energy on the cutoff for the bosonic system.

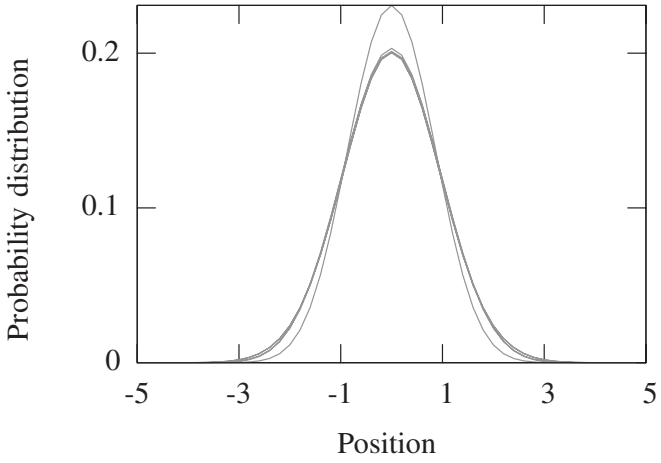

FIG. 3. The dependence of the space distribution of the bosonic ground state on the cutoff N_{cut}, for N_{cut} equal 16 (highest curve), 36, 64, 128 (lowest curve).

cutoffs. The convergence is reached for $N_{\text{cut}} = 128$. The free parameters were chosen as $I = [-5, 5]$ and $\epsilon = 0.01$. Obviously these values are only exemplary and can be tuned at will.

IV. SYMMETRIES OF THE SYSTEM

A. Bosonic case and the C_{4v} group

The Hamiltonian of the quantum bosonic system (1) is invariant with respect to a point group of symmetries, which consists of a 4-fold principal axis of symmetry and four reflection axes perpendicular to the principal axis, and is called the C_{4v} group. It has eight elements:

e	identity,
π_x	reflection with respect to the x axis ,
π_y	reflection with respect to the y axis ,
$\pi_{x=y}$	reflection with respect to the $x = y$ line ,
$\pi_{x=-y}$	reflection with respect to the $x = -y$ line ,
$R_{\pi/2} \equiv R$	rotation through the angle of $+\frac{\pi}{2}$ radians,
$R_{\pi} \equiv R^2$	rotation through the angle of $+\pi$ radians,
$R_{3\pi/2} \equiv R^3$	rotation through the angle of $+\frac{3\pi}{2}$ radians

We call a conjugacy class a subset of all elements of a group G that commute with all elements of G. The group C_{4v} has five conjugacy classes:

$$id = \{e\}, \qquad 2C_4 = \{R, R^3\}, \qquad C_2 = \{R^2\},$$
$$2S_v = \{\pi_x, \pi_y\}, \qquad 2S_d = \{\pi_{x=y}, \pi_{x=-y}\}.$$

It is known [13], that the number of irreducible representations of a group is equal to the number of classes of this group. At the same time, the sum of squares of dimensions of this representations must be equal to the order of the group. All this implies that C_{4v} must have four 1-dimensional and one 2-dimensional irreducible representations. The defining representation is 2-dimensional and is explicitly shown in (16). Each group has also a 1-dimensional, trivial representation composed of ones.

$$e = \begin{pmatrix} 1 & 0 \\ 0 & 1 \end{pmatrix}, \qquad R = \begin{pmatrix} 0 & 1 \\ -1 & 0 \end{pmatrix},$$
$$R^2 = \begin{pmatrix} -1 & 0 \\ 0 & -1 \end{pmatrix}, \qquad R^3 = \begin{pmatrix} 0 & -1 \\ 1 & 0 \end{pmatrix},$$
$$\pi_x = \begin{pmatrix} -1 & 0 \\ 0 & 1 \end{pmatrix}, \qquad \pi_y = \begin{pmatrix} 1 & 0 \\ 0 & -1 \end{pmatrix}, \tag{16}$$
$$\pi_{x=y} = \begin{pmatrix} 0 & 1 \\ 1 & 0 \end{pmatrix}, \qquad \pi_{x=-y} = \begin{pmatrix} 0 & -1 \\ -1 & 0 \end{pmatrix}.$$

In order to find the remaining three 1-dimensional representations, one uses a couple of observations. First, every representation of the identity element has to be equal 1. Second, except the elements of the $2C_4$ class, all elements squared give the identity element. Thus, their representations must be equal $+1$ or -1. Moreover, one can obtain the elements of the C_2 class by combining the elements of the classes $2C_4$, $2S_v$, and $2S_d$ (i.e. reflection with respect to the OX axis and a reflection with respect to the OY axis give a rotation through an angle of π). So the representations of the C_2 class must be equal to $+1$. As the representations of the $2C_4$ class are concerned, they can be equal $+1$ or -1, because when squared they must give the elements of the C_2 class. In order that the multiplication table remains unchanged the representations equal to -1 must appear in pairs. All these observations permit to identify all 1-dimensional representations of the C_{4v} group (Table I). The eigenstates transform according to one of the irreducible representation. We have four 1-dimensional representations, A_1, A_2, B_1, and B_2, so we will have four series of nondegenerate states. States transforming according to the representation E will be doubly degenerate. A state symmetric with respect to three reflections π_x, π_y, and $\pi_{x=y}$ will transform according to the trivial representation A_1. A state symmetric with respect to π_x and π_y reflections but antisymmetric with respect to $\pi_{x=y}$ will transform according to the B_1 representations. Table II contains first twelve states, their symmetries, and the representation they belong to.

TABLE I. Four 1-dimensional irreducible representations of the C_{4v} group.

	e	$2C_4$	C_2	$2S_v$	$2S_d$
A_1	1	1	1	1	1
A_2	1	1	1	-1	-1
B_1	1	-1	1	1	-1
B_2	1	-1	1	-1	1

TABLE II. First 12 eigenstates of the quantum bosonic system with a corresponding representation of the symmetry group C_{4v}. In the column entitled "Energy" the exact energies are shown, whereas the "B-O" column contains values calculated in the Born-Oppenheimer approximation. In the columns from 4 to 10 are shown the parity or a lack of a given symmetry for each state.

State	Energy	B-O	π_x	π_y	$\pi_{x=y}$	$\pi_{x=-y}$	R	R^2	R^3	Representation
1	1.1082	1.1737	+	+	+	+	+	+	+	A_1
2	2.3788	2.3381	−	+	0	0	0	−	0	E
3	2.3788	2.4414	+	−	0	0	0	−	0	E
4	3.0574	3.2711	+	+	−	−	−	+	−	B_1
5	3.5229	3.4319	+	+	+	+	+	+	+	A_1
6	4.1100	4.0878	+	−	0	0	0	−	0	E
7	4.1100	4.2950	−	+	0	0	0	−	0	E
8	4.8210	4.8307	+	+	−	−	−	+	−	B_1
9	5.0113	4.8635	−	−	+	+	−	+	−	B_2
10	5.1120	5.0783	+	+	+	+	+	+	+	A_1
11	5.6947	5.5206	+	−	0	0	0	−	0	E
12	5.6947	5.8053	−	+	0	0	0	−	0	E

B. Supersymmetric case

The quantum supersymmetric Hamiltonian remains unchanged under action of transformations which form the following group:

e	identity ,	
$\tilde{\pi}_x$	$x \to -x$,	$y \to y$,
	$f \to -f^\dagger$,	$f^\dagger \to -f$,
$\tilde{\pi}_y$	$x \to x$,	$y \to -y$,
	$f \to f^\dagger$,	$f^\dagger \to f$,
$\tilde{R}_\pi$	$x \to -x$,	$y \to -y$,
	$f \to -f$,	$f^\dagger \to -f^\dagger$,
$\tilde{\pi}_{x=y}$	$x \to y$,	$y \to x$,
	$f \to if^\dagger$,	$f^\dagger \to -if$,
$\tilde{\pi}_{x=-y}$	$x \to -y$,	$y \to -x$,
	$f \to -if^\dagger$,	$f^\dagger \to if$,
$\tilde{R}_{\pi/2}$	$x \to -y$,	$y \to x$,
	$f \to if$,	$f^\dagger \to -if^\dagger$,
$\tilde{R}_{3\pi/2}$	$x \to y$,	$y \to -x$,
	$f \to -if$,	$f^\dagger \to if^\dagger$

The aim of this notation is to highlight the similarity of the above group and the C_{4v} group. In this spirit we call this group the $\tilde{C}_{4v}$ group. We again find five conjugacy classes:

$$id = \{e\}, \qquad 2\tilde{C}_4 = \{\tilde{R}_{\pi/2}, \tilde{R}_{3\pi/2}\}, \qquad \tilde{C}_2 = \{\tilde{R}_\pi\},$$
$$2\tilde{S}_v = \{\tilde{\pi}_x, \tilde{\pi}_y\}, \qquad 2\tilde{S}_d = \{\tilde{\pi}_{x=y}, \tilde{\pi}_{x=-y}\}.$$

We can perform a similar analysis as in the bosonic case and obtain four 1-dimensional and one 2-dimensional irreducible representations [Table III and formula (17)]:

$$e = \begin{pmatrix} 1 & 0 \\ 0 & 1 \end{pmatrix}, \qquad \tilde{\pi}_x = \begin{pmatrix} -1 & 0 \\ 0 & 1 \end{pmatrix},$$
$$\tilde{\pi}_y = \begin{pmatrix} 1 & 0 \\ 0 & -1 \end{pmatrix}, \qquad \tilde{R}_\pi = \begin{pmatrix} -1 & 0 \\ 0 & -1 \end{pmatrix},$$
$$\tilde{\pi}_{x=y} = \begin{pmatrix} 0 & 1 \\ 1 & 0 \end{pmatrix}, \qquad \tilde{\pi}_{x=-y} = \begin{pmatrix} 0 & -1 \\ -1 & 0 \end{pmatrix},$$
$$\tilde{R}_{\pi/2} = \begin{pmatrix} 0 & -1 \\ 1 & 0 \end{pmatrix}, \qquad \tilde{R}_{3\pi/2} = \begin{pmatrix} 0 & 1 \\ -1 & 0 \end{pmatrix}. \tag{17}$$

Since all elements of the $\tilde{C}_{4v}$ group commute with the Hamiltonian, one can choose one of these symmetries in order to define an additional quantum number. Let us choose the following:

$$\tilde{\pi}_y: x \to x, \qquad y \to -y, \qquad f \to f^\dagger, \qquad f^\dagger \to f.$$

The action of $\tilde{\pi}_y$ on basis vectors is given by

$$\tilde{\pi}_y |n_x, n_y, n_f\rangle = (-)^{n_y} |n_x, n_y, 1 - n_f\rangle.$$

One can define even and odd states with respect to $\tilde{\pi}_y$:

$$|n_x, n_y, \pm\rangle = \frac{1}{\sqrt{2}}(|n_x, n_y, 0\rangle \pm (-)^{n_y} |n_x, n_y, 1\rangle.$$

In such a basis the Hamiltonian appears as a block diagonal matrix with two sectors, and it is possible to diagonalize each block independently. Although we have introduced a

TABLE III. Four 1-dimensional irreducible representations.

	e	$2\tilde{S}_v$	$\tilde{C}_2$	$2\tilde{C}_4$	$2\tilde{S}_d$
A	1	1	1	1	1
B	1	−1	1	1	−1
C	1	1	1	−1	−1
D	1	−1	1	−1	1

TABLE IV. Eight first energies for three different cutoffs for the supersymmetric case. The degeneracy due to the point symmetries is exact for each cutoff.

	$N_{\text{cut}} = 72$	$N_{\text{cut}} = 128$	$N_{\text{cut}} = 200$
1	0.2871	0.2469	0.1788
2	0.2871	0.2469	0.1788
3	1.2172	0.8573	0.7553
4	1.2172	0.8573	0.7553
5	2.2215	1.8932	1.5014
6	2.2215	1.8932	1.5014
7	3.1867	2.7090	2.4616
8	3.1867	2.7090	2.4616

squared cutoff, the basis remains invariant with respect to the symmetries from the $\tilde{C}_{4v}$ group. The spectrum of the supersymmetric system (2) will have degeneracies due to these symmetries for each cutoff. It turns out that all states transform according to the 2-dimensional irreducible representation, so they will all be doubly degenerate. Table IV shows eight first energies for three different cutoffs.

C. Supersymmetry

Supersymmetry can manifest itself in a given quantum system through the set of supersymmetry generators, which form a well-defined algebra, or, on a more experimental level, through a characteristic structure (degeneracies) of the spectrum. In this paper we assume that the existence of a single ground state with zero energy and supersymmetric doublets of higher energies guarantees the presence of supersymmetry. Indeed, in the case of system (2) the generators Q and $Q^\dagger$ do not fulfill all relations of a supersymmetry algebra, namely $Q^2 \neq 0$. Moreover, Q does not conserve the bosonic occupation number, so the introduction of the cutoff breaks the supersymmetry and destroys its fingerprints on the spectrum. One expects its restoration in the limit $N_{\text{cut}} \to \infty$. However, there exists a way of establishing the supersymmetry for each finite N_{cut}. One can remark, that, since Q is Hermitian, the Hamiltonian (2) is a product of generators Q specified for an infinite cutoff, and then cut to the desired dimensions. On the other hand, one can conceive the Hamiltonian matrix as a product of matrices of already cut generators Q:

$$[H_{\text{susy}}] = [Q_{\text{finite } N_{\text{cut}}}][Q_{\text{finite } N_{\text{cut}}}]. \tag{18}$$

Of course, the Hamiltonians (2) and (18) agree in the limit of infinite cutoff. It turns out that the spectrum of (18) is fully supersymmetric. A sample of results for three different cutoffs are shown in Table V. One can observe a double degeneracy due to the point symmetries of the system, as well as a supersymmetric degeneracy. Moreover, one can notice in Table V yet another way of supersymmetry breaking. For square cutoffs with $N_{\text{cut}}/2$ even, the spectrum cannot contain a single ground state and $N_{\text{cut}}/4 - 1$ supersymmetric doublets. In such a situation the supersymmetry is broken and the ground state disappears.

TABLE V. Twelve first eigenvalues of the matrix $[H_{\text{susy}}]$ for three different cutoffs. The degeneracies have two origins: supersymmetry and point symmetries of the group $\tilde{C}_{4v}$. For cutoff, for which $N_{\text{cut}}/2$ is even, the supersymmetry is broken and the spectrum does not have the zero energy ground state.

$N_{\text{cut}} = 50$	$N_{\text{cut}} = 200$	$N_{\text{cut}} = 450$
0.0000	0.0165	0.0000
0.0000	0.0165	0.0000
	0.0165	
	0.0165	
0.3371	0.3607	0.0862
0.3371	0.3607	0.0862
0.3371	0.3607	0.0862
0.3371	0.3607	0.0862
1.0163	0.8867	0.3760
1.0163	0.8867	0.3760
1.0163	0.8867	0.3760
1.0163	0.8867	0.3760

V. QUANTUM SYSTEMS

In this section we will compare the numerical spectra of the bosonic and supersymmetric quantum system.

A part of the spectrum of the bosonic system (1) is shown in Fig. 4. The dependence of twelve first eigenenergies on the cutoff is depicted. Numerical values are presented in Table II. Consequently, to the discussion of the symmetries of the system, the spectrum contains four nondegenerate series of states and one doubly degenerate. The degeneracies due to the point symmetries are present for each N_{cut}, because the cutoff does not spoil them. After the paper [14], the dependence of the eigenenergy on the cutoff enables one to decide whether the state belongs to the

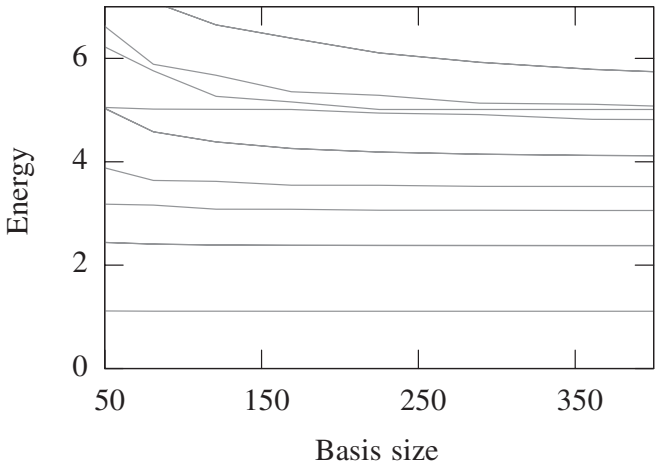

FIG. 4. The dependence of the 12 first eigenenergies on the cutoff for the bosonic case.

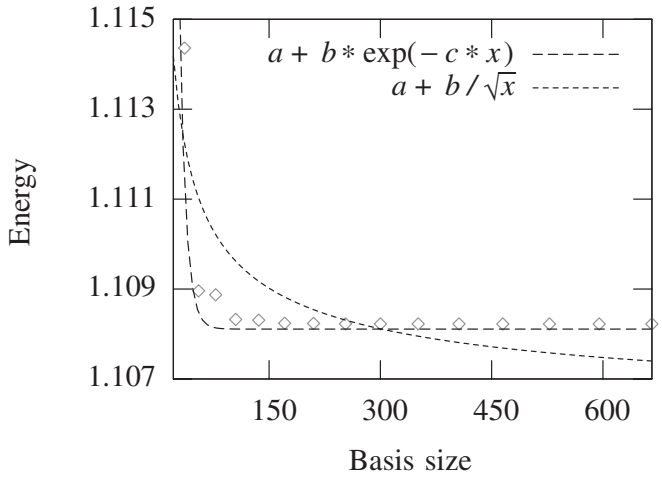

FIG. 5. The dependence of the bosonic ground state energy on the cutoff with fitted curves: an exponential one and an inverse square root.

discrete spectrum or to the continuous one. If the dependence on N_{cut} is of the type $\frac{1}{N_{\text{cut}}}$ or slower, then the corresponding state is a nonlocalized state from the continuous spectrum. Contrary, if the dependence is fast, for example, exponential $\sim e^{-N_{\text{cut}}}$, then the state is localized. Figure 5 shows the dependence of the bosonic ground state on the cutoff and two fitted curves: an exponent $f(N_{\text{cut}}) = a + be^{-cN_{\text{cut}}}$ and an inverse square root $g(N_{\text{cut}}) = a + b/\sqrt{N_{\text{cut}}}$. The first one fits much better which means that the ground state is localized. It turns out that all other states analyzed with this method belong also to the discrete spectrum. This is also confirmed by an analysis of the virial, which is a scalar product of vectors of momentum and position $w = \vec{p} \cdot \vec{x}$. In the classical regime, the mean time derivative of a virial tends to zero on a bounded trajectory and explodes on an unbounded one. On the

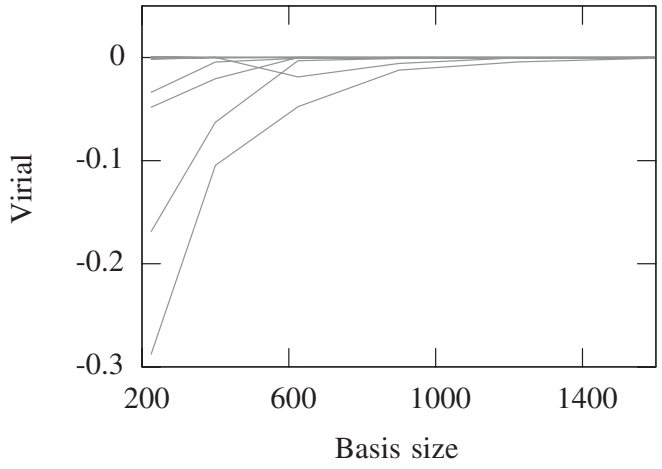

FIG. 6. The dependence of the quantum virial on cutoff for ten first bosonic states. The convergence for the ground state is the fastest. The most distant from zero curve corresponds to the tenth eigenstate.

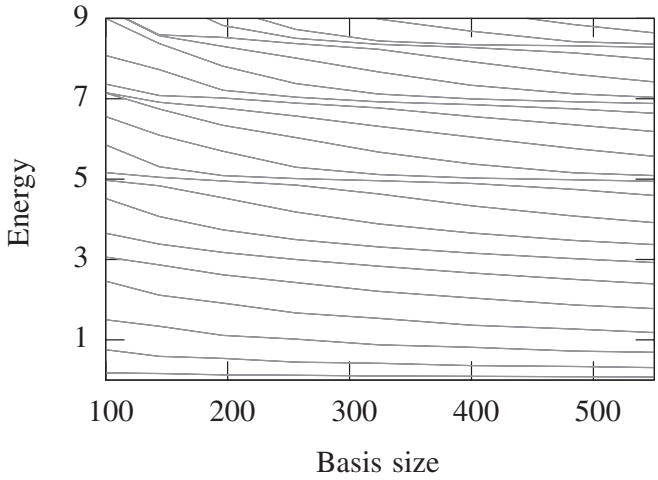

FIG. 7. The dependence of the 32 first states on the cutoff for the supersymmetric case.

quantum level, the evaluation of the expectation value of a corresponding operator in a given state can supply a similar type of information. In the bosonic case, one is left with the following expression:

$$\langle \dot{w}_{\text{bosonic}} \rangle = 2(\langle \hat{p}_x^2 \rangle + \langle \hat{p}_y^2 \rangle - 2\langle \hat{x}^2 \hat{y}^2 \rangle). \tag{19}$$

The results for ten first states are shown in Fig. 6 as a function of cutoff. We notice that all values converge to zero, which confirms that the bosonic states are localized.

On the other hand, the supersymmetric spectrum is shown in Fig. 7. According to the symmetries of the system, all states are doubly degenerate due to the point symmetries from the $\tilde{C}_{4v}$ group. The supersymmetric degeneracy can be found in the infinite cutoff limit. The fitted cutoff dependence of the supersymmetric ground state is shown in Fig. 8 and suggests that it is a nonlocalized state. The analysis of higher states also confirms that they belong

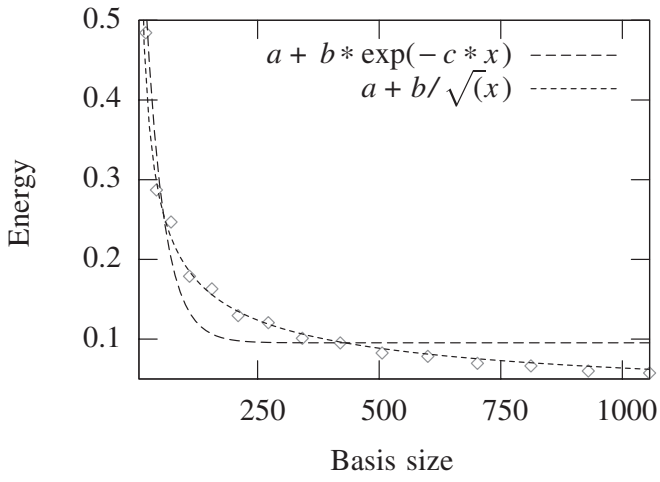

FIG. 8. The dependence of the supersymmetric ground state energy on the cutoff with fitted curves: an exponential one and an inverse square root.

to the continuous spectrum. Thus, it seems that the spectrum of the quantum supersymmetric system is composed of purely nonlocalized states. But, the approximate solution of the supersymmetric model (4) indicates that among them one might find localized states from the discrete spectrum. And indeed we have found such states in the numerical spectrum of the exact Hamiltonian (2). However, as their convergence is exponential we may expect that they should cross states with slower cutoff dependence. The rules of quantum mechanics claim that, when a parameter in a Hamiltonian is changed, the states of the same symmetry cannot cross. In our case, such a parameter is our cutoff, and as was mentioned, all states transform according to the 2-dimensional irreducible representation of the $\tilde{C}_{4v}$ group. So these localized states must have an interesting realization. One can see them in Fig. 7 as deformations of the energy dependence on the cutoff. More precisely, there exist states which on some interval N_{cut} have a constant energy (i.e. the deformations for energies around $E = 5$). If the energy of such a state remained unchanged till some cutoff $\tilde{N}_{\mathrm{cut}}$, then for $N_{\mathrm{cut}} > \tilde{N}_{\mathrm{cut}}$ it starts decreasing as $\frac{1}{N_{\mathrm{cut}}}$. However, from $\tilde{N}_{\mathrm{cut}}$ the energy of the higher, neighboring state assumes this value (here $E = 5$) and remains constant on some adjacent interval. In this way localized states coexist with nonlocalized ones in the same range of energy. These results can again be confirmed by the virial analysis. We have to evaluate the operator,

$$\langle \dot{w}_{\mathrm{susy}} \rangle = 2\langle \hat{p}_x^2 \rangle + 2\langle \hat{p}_y^2 \rangle - 4\langle \hat{x}^2 \hat{y}^2 \rangle - \langle \sigma_x \hat{x} \rangle + \langle \sigma_y \hat{y} \rangle. \tag{20}$$

In Fig. 9 the time derivative of virial for four supersymmetric states is depicted as a function of the cutoff. For a majority of them the obtained values are far from 0. These states are nonlocalized. However, as was observed there can exist also some localized states. Taking into account their realization through many nonlocalized states, one concludes that the states for which the quantum virial has a value near 0 for a given cutoff, are just the states that form the localized state.

To summarize, the main observation is that bosonic and supersymmetric eigenstates have a different character. The first ones are localized and thus belong to the discrete spectrum, whereas the supersymmetric spectrum is composed from both types of states. This disparity is essential in the following discussion.

VI. CLASSICAL SYSTEMS

The differences in the behavior of classical bosonic and supersymmetric trajectories are striking at the first glance. Similarly, as in the quantum regime the bosonic states were localized and the supersymmetric were nonlocalized, the bosonic trajectories are bounded, and the supersymmetric escape through the flat directions of the potential.

More precisely, the numerical solutions of bosonic equations of motions (7) show that all investigated trajectories

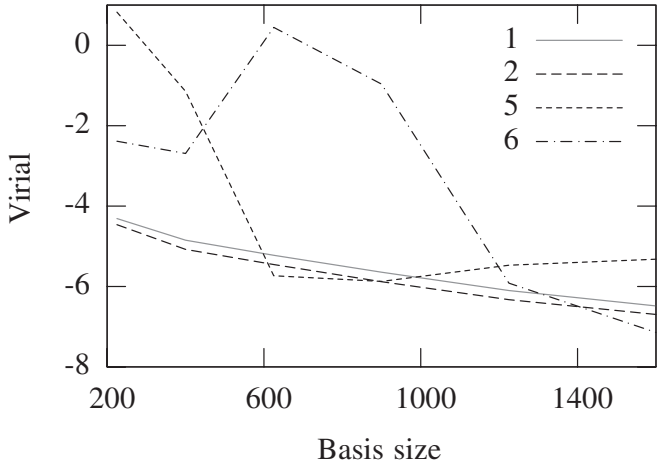

FIG. 9. The dependence of the quantum virial on the cutoff for some selected supersymmetric states (first, second, fifth, and sixth).

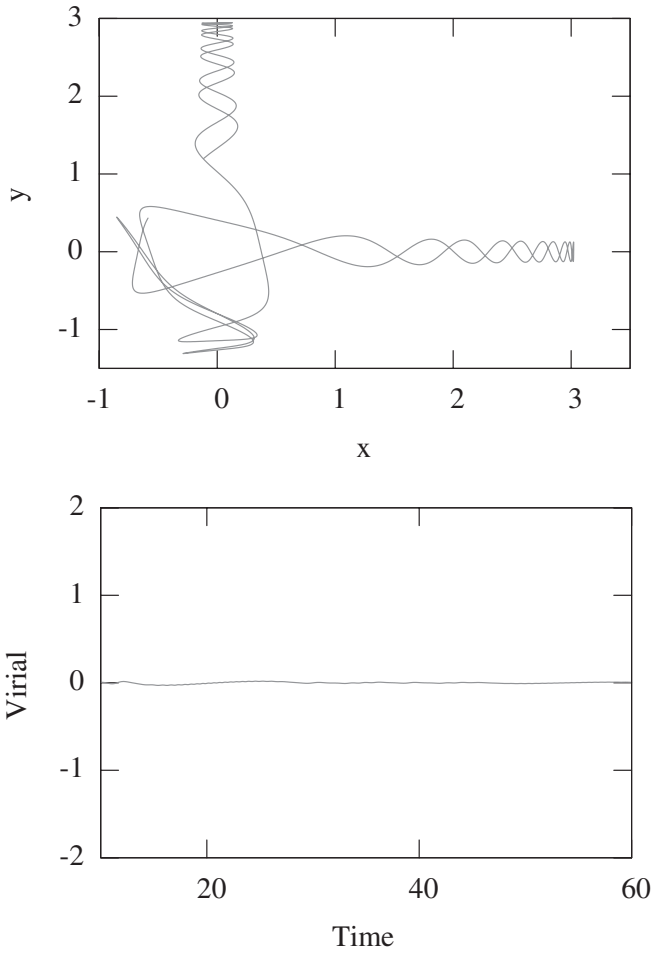

FIG. 10. An exemplary bosonic classical trajectory and the virial dependence on time. The mean time derivative of the virial has small values indicating that the trajectory is bounded.

are bounded. They all come back to the center of the potential. Similarly, as in the case of the hyperbolic billiard potential, mentioned earlier, only particles that move along the coordinate axes can escape through the valleys. In the quantum regime, we used the virial theorem to decide whether quantum states were localized or not. Now, we would like to do the same using the classical virial theorem. It implies that for a bounded motion (with finite momentum and position) in a potential that vanishes as $\frac{1}{r}$, one has

$$0 = \frac{\overline{dw}}{dt} = \bar{U} + 2\bar{K}, \tag{21}$$

where w is the virial, $\frac{d}{dt}$ is the time derivative, $\bar{\cdot}$ stands for the time averaging, U is the potential energy, and K is the kinetic energy. In order to verify the character of the classical trajectories, one needs to evaluate the quantity (21) on a given trajectory. A representative bosonic trajectory and the corresponding plot of the virial are shown in Fig. 10. The mean time derivative of the virial remains near zero, which indicates that the trajectory is bounded. Moreover, using the algorithm proposed by Schmelcher and Diakonos [15] we found some closed orbits, one of which is shown in Fig. 11. Investigation of eigenvalues of the Jacobian shows that this orbit is unstable. It is worth noting that similar research was made by Dalhqvist and Russberg [16], who found a stable island in the phase space of the x^2y^2 potential, therefore showing that the latter is not ergodic as was believed.

On the contrary, all supersymmetric trajectories escape through the valleys of potential. However, there exist some of them which for a large amount of time remain in the center of potential. When the dependence of the number of returns of some trajectory on its energy is investigated, one finds sharp peaks suggesting that there exist trajectories with a huge number of returns. Again, we found one unstable closed orbit using the Schmelcher's algorithm, shown in Fig. 11. The virial theorem confirms the unbounded character of supersymmetric trajectories. The evaluation of (21) for a given trajectory shows that the value of the time derivative of the virial explodes as the

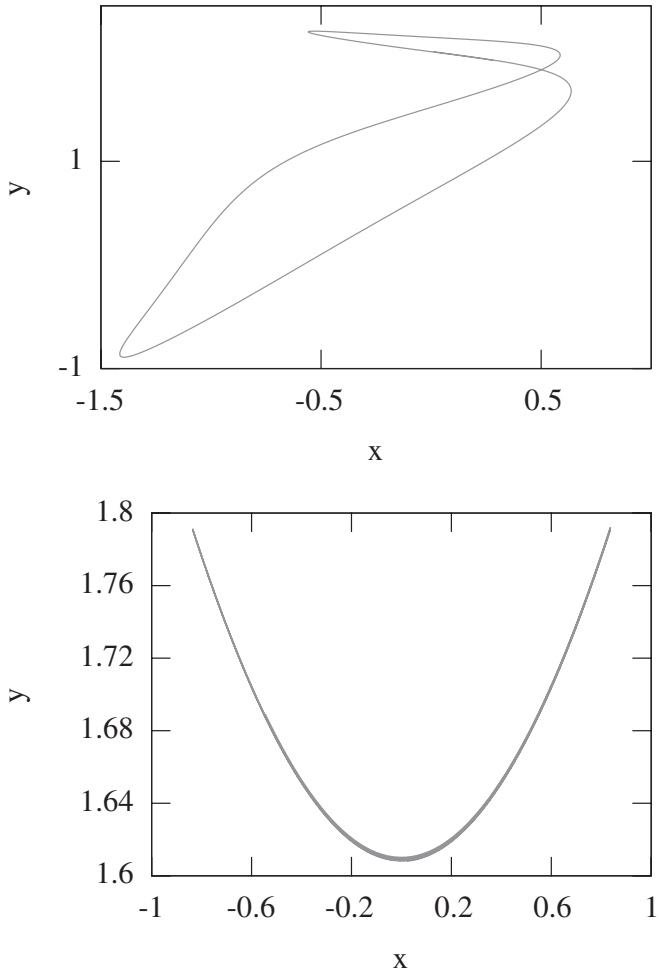

FIG. 11. Closed bosonic and supersymmetric orbits.

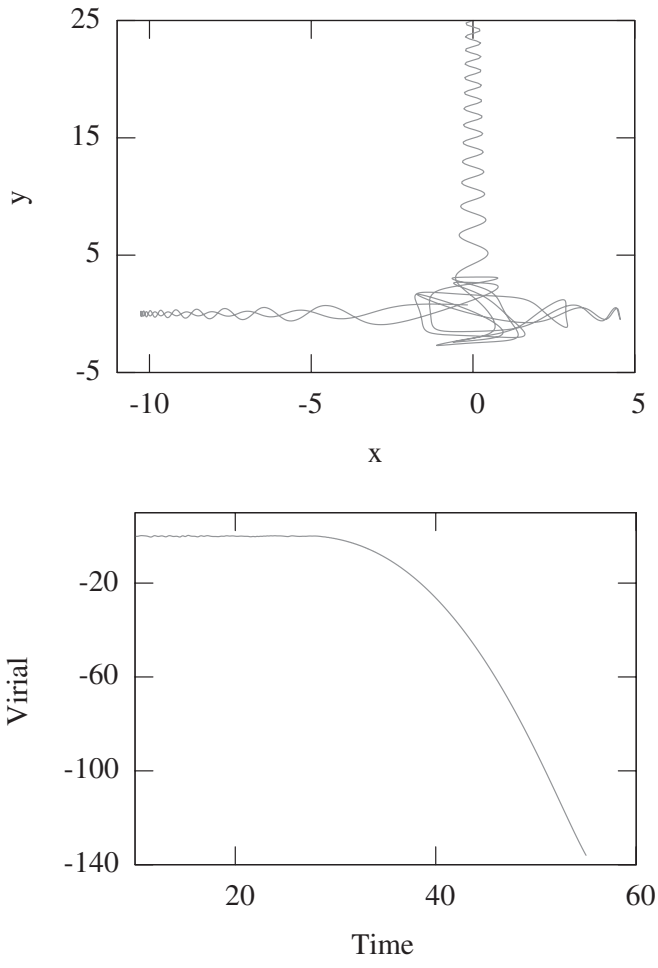

FIG. 12. An exemplary supersymmetric classical trajectory and the virial dependence on time. The mean time derivative of the virial explodes when the particle escapes through the valley.

particle escapes through the valley. Figure 12 depicts these results.

The findings obtained in this part show that the behavior of classical trajectories and quantum states is analogous. For the bosonic system quantum states are localized and classical trajectories are bounded. On the contrary, for the supersymmetric case, the majority of states are nonlocalized. The corresponding classical motion is a trajectory which escapes through the valleys. The localized supersymmetric quantum states are accompanied by closed classical orbits. So, the differences observed between quantum systems are also found on the classical level. This pattern might indicate the existence of classical manifestation of supersymmetry.

VII. CONCLUSION

In this paper we investigated the properties of a system proposed by de Wit, Lüscher, and Nicolai, in both quantum and classical regimes. By comparing it with the bosonic system we observed several interesting facts.

We started by introducing the quantum Hamiltonians of the bosonic and supersymmetric systems with the potential with four flat valleys. Using the Born-Oppenheimer approximation, we succeeded in solving both systems. We concluded that a bosonic quantum particle moving in one of the valleys is exposed to an effective potential barrier which prevents it from escaping. Thus, all states are localized. Contrary, the supersymmetric quantum particle can enter at any depth into the valleys. The supersymmetric spectrum consists of states from the continuous spectrum and, coexisting with them, some localized states. Then, we introduced the Hamiltonians of the classical counterparts of these systems. For the supersymmetric system, we obtained the equations of motion which describe a particle with spin which precess around some vector field. The interesting feature is that this field is tangent to the contour lines of the potential. Next, we described the cutoff method and some criteria for testing the reliability of numerical results. The symmetries of considered systems, discussed subsequently, fully explain all degeneracies of exact energies. The comparison of the bosonic and supersymmetric spectra confirmed the hypothesis based on the approximated solutions on the character of quantum states. We observed the noteworthy realization of the supersymmetric localized states as deformations of the energy dependence on the cutoff. We then turned our attention to the classical regime. We described the behavior of trajectories of the classical bosonic and supersymmetric systems. It turned out that the character of the trajectories corresponds to the character of quantum states. Bosonic trajectories are bounded, whereas the supersymmetric ones escape through the valleys of the potential which can be due to the spin precession. The above results show that the differences between quantum states are also present on the classical level.

The supersymmetric potentials with flat directions appear also in some much more sophisticated physical problems, i.e. in systems connected with supersymmetric Yang-Mills quantum mechanics (SYMQM). The investigated system is one of the simplest models possessing many of the properties of SYMQM. A deeper analysis can help to understand, for example, the coexistence of the continuous and discrete spectrum in these systems. Moreover, the surprising effect of spin precession on the motion of a classical, supersymmetric particle which enables it to escape through the flat directions deserves further attention.

ACKNOWLEDGMENTS

I would like to thank Professor J. Wosiek for invaluable help with this paper. This work is partially supported by Grant No. P03B 024 27 (2004–2007) of the Polish Ministry of Education and Science.

[1] J. Wosiek, Nucl. Phys. **B644**, 85 (2002).
[2] M. Campostrini and J. Wosiek, Phys. Lett. B **550**, 121 (2002).
[3] M. Campostrini and J. Wosiek, Nucl. Phys. **B703**, 454 (2004).
[4] T. Banks, W. Fischler, S. H. Shenker, and L. Susskind, Phys. Rev. D **55**, 5112 (1997).
[5] B. de Wit, M. Lüscher, and H. Nicolai, Nucl. Phys. **B320**, 135 (1989).
[6] H. Nicolai and R. Helling, hep-th/9809103.
[7] R. Helling, hep-th/0009134.
[8] C. C. Mertens, R. L. Waterland, and W. P. Reinhardt, J. Chem. Phys. **90**, 2328 (1989).
[9] F. Cooper, A. Khare, and U. Sukhatme, Phys. Rep. **251**, 267 (1995).
[10] M. Sieber and F. Steiner, Physica D (Amsterdam) **44**, 248 (1990).
[11] F. A. Berezin and M. S. Marinov, Ann. Phys. (Leipzig) **104**, 336 (1977).
[12] P. Jordan and E. P. Wigner, Z. Phys. **47**, 631 (1928).
[13] H. Georgi, *Lie Algebras in Particle Physics* (Perseus Books, Reading, MA, 1999).
[14] M. Trzetrzelewski and J. Wosiek, Acta Phys. Pol. B **35**, 1615 (2004).
[15] D. Pingel, P. Schmelcher, and F. K. Diakonos, Phys. Rev. E **64**, 026214 (2001).
[16] P. Dahlqvist and G. Russberg, Phys. Rev. Lett. **65**, 2837 (1990).